

**Link sito dell'editore:** <https://www.sciencedirect.com/science/article/pii/S0263224116305206>

**Link codice DOI:** <https://doi.org/10.1016/j.measurement.2016.09.017>

**Citazione bibliografica dell'articolo:**

Andrea Cataldo, Egidio De Benedetto, Giuseppe Cannazza, Antonio Masciullo, Nicola Giaquinto, Giuseppe Maria D'Aucelli, Nicola Costantino, Antonio De Leo, Marcello Miraglia, "Recent advances in the TDR-based leak detection system for pipeline inspection", pubblicato in *Measurement*, 2017, Vol. 98, pag. 347-354,

# Recent advances in the TDR-based leak detection system for pipeline inspection

Andrea Cataldo<sup>a</sup>, Egidio De Benedetto<sup>a</sup>, Giuseppe Cannazza<sup>a</sup>, Antonio Masciullo<sup>a</sup>, Nicola Giaquinto<sup>b</sup>, Giuseppe Maria D'Aucelli<sup>b</sup>, Nicola Costantino<sup>c</sup>, Antonio De Leo<sup>d</sup>, Marcello Miraglia<sup>d</sup>

<sup>a</sup>University of Salento - Department of Engineering for Innovation, Complesso Ecotekne, via Monteroni, 73100 Lecce, Italy

<sup>b</sup>Polytechnic of Bari - Department of Electrical and Information Engineering, Bari, Italy,

<sup>c</sup>Polytechnic of Bari - Department of Mechanics Mathematics and Management, Bari, Italy,

<sup>d</sup>Acquedotto Pugliese S.p.A., Bari, Italy

---

## Abstract

In this paper, the most recent advances in the time-domain reflectometry (TDR)-based system for leak-localization in underground pipes are described in detail. More specifically, a new design of sensing element and the use of a new connection modality are proposed. Thanks to these new features, the practical implementation of the system becomes much quicker and its use more effective.

Additionally, the present work also describes all the practical aspects and technical details (from installation to functional tests), related to the practical implementation of the system.

Finally, to assess the possibility of further increasing the cost-effectiveness of the TDR-based leak localization system, experimental tests were carried out by comparatively using two TDR instruments, differing in specifications and costs, to identify the position of a leak.

*Keywords:* leak detection, leak localization, time domain reflectometry, water pipes, water leakage

---

## 1. Introduction

The problem of leakages in public water systems seriously undermines water-resource efficiency [1]. Therefore, the localization of leaks in underground pipes is one of the crucial steps for the optimization of the use of water resources [2], as leakage is usually the largest component of distribution loss [3]. Also, considering that water availability is already under pressure across Europe (as one fifth of Europe's population live in Countries where the total water abstraction is threatening the availability of water resources); this aspect should be taken in particular consideration by Member States as an important element of measures to achieve the objectives of the Water Frame Directive [4]. To give a rough idea of the issue, water loss from a single circular hole with 6 mm diameter in a distribution pipe at 60 m pressure amounts to 1.8 m<sup>3</sup> per hour or 1300 m<sup>3</sup> per month [5].

A comprehensive review of inspection technologies for condition assessment of water pipe can be found in [6]. The most widespread leak-detection systems rely on acoustic techniques, and are based on the propagation of mechanical waves. Traditional acoustic leak-detection systems include listening rods, leak correlators, and noise loggers [7]. Despite the extensive use of these systems, their performance depends on the material and diameter of the pipes; also, it can be severely compromised in case of low hydraulic pressure in the pipes, in presence of high environmental acoustic noise, in case of unsuitable sound propagation conditions, etc. [8].

On such bases, recently, an innovative time domain reflectometry (TDR)-based system for the localization of leaks in underground pipes has been developed by the Authors [9, 10]. Because this system is based on the propagation of electromagnetic (EM) waves (rather than acoustic waves), it overcomes most of the limitations that typically affect the performance of traditional leak detection systems. The developed TDR-based system is not influenced by any of the aforementioned limitations that affect traditional, acoustic leak-detection techniques. In particular, the TDR-based system can be used to localize leaks on pipes made

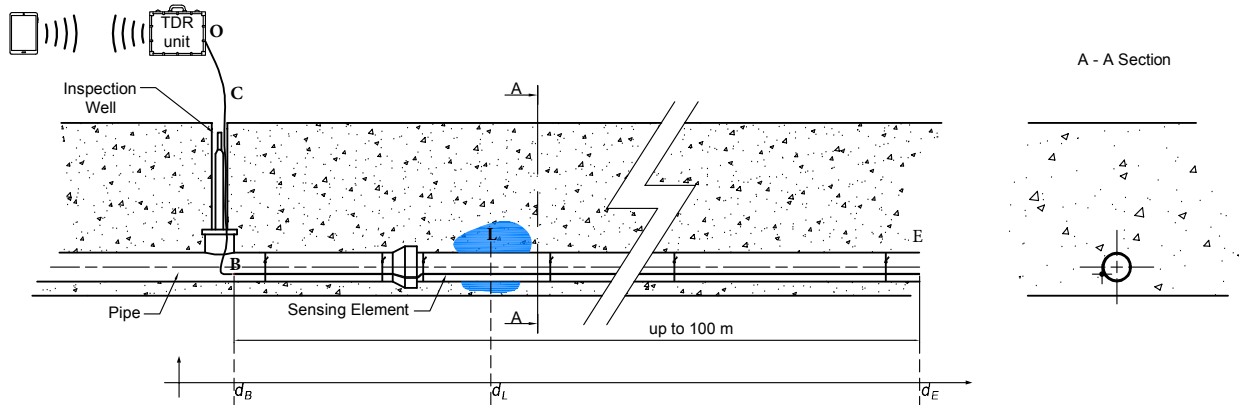


Figure 1: Schematization of the measurement apparatus for the TDR-based leak localization in underground pipes.

of any material and also on non-pressurized pipes: these aspects make it a viable solution also for leak detection in sewer pipes.

Fig. 1 shows a simplified schematization of the TDR-based measurement apparatus. The proposed system requires that, during the installation of new pipes, a wire-like sensing element (SE) be buried along the pipe to be monitored. The SE is laid on the pipe and remains permanently buried with it. The beginning of the SE is connected to a cable, which emerges through an inspection well. When an operator has to check for the possible presence of leaks, it suffices to connect the TDR measurement instrument to the beginning of the SE, and the system provides in real time the position of the leak. Each single SE can be up to 100 m-long and can follow the topology of the pipe network.

The effectiveness of the this TDR-based system has been demonstrated through an extensive experimental campaign carried out on several pilot plants [10]. As reported in [11], recently, this system has been installed on 10 km of underground water pipes, by the Acquedotto Pugliese S.p.A. (the largest European water operator).

On the basis of the promising results of the large-scale implementation of this system, the present work describes the major recent advances of the TDR-based leak localization system, that have been introduced to expedite the installation phase and to make the leak-detection activity even more effective.

The first enhancement pertains to the adoption of a SE configuration that is different from the one adopted previously [10]. As will be detailed later on in this paper, the choice of a different configuration for the SE allows avoiding the design phase (prior to the installation), in which it was necessary to pre-establish the optimal positioning of the SE's and their length [11].

An additional enhancement consists in the introduction of a new modality for the electrical connection of the TDR instrument to the beginning of the SE (i.e., housed in the inspection well of Fig. 1). In the previous configuration of the TDR-based system, in fact, it was necessary to include a plastic box (inside the inspection well) for protecting the electrical connectors from the environment [11]. In this work, the use of the protecting plastic box has been avoided by resorting to an ingress protected (IP) electrical connector. Additionally, it will be shown that, thanks to the presence of five pins, one single connector can be used for different type of measurements.

Finally, to further increase the cost-effectiveness of the TDR-based leak localization system in view of large-scale implementation, the possibility of employing lower-cost TDR instrument was also addressed. To this purpose, two TDR instruments (with different specifications and costs) were comparatively employed to localize the position of a leak, and their performance was assessed.

This paper is structured as follows. In Section 2, the theoretical background at the basis of the TDR-based leak localization system is provided. In Section 3, the enhancement features brought to the system are

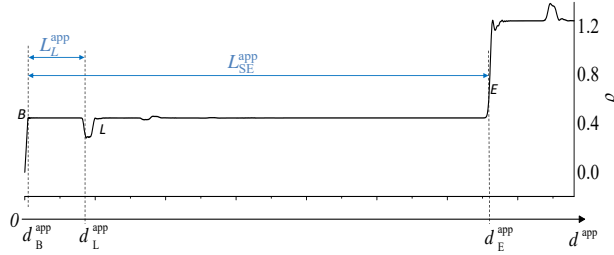


Figure 2: Schematization of a possible TDR reflectogram, in presence of a leak, when the TDR signal is a step-like voltage signal.

described in detail. In Section 4, all the steps for the implementation and use of the leak-localization system are thoroughly described. In Section 5, the experimental results related to the comparative assessment of the performance of two TDR instruments in localizing the leaks are reported. Finally, in Section 6, conclusions are drawn.

## 2. Background and description of the measurement apparatus

TDR was originally developed mainly for the localization of faults in electric wires [12]; however, thanks to its adaptability, TDR has progressively established itself as an appealing solution in the most diverse application contexts, such as moisture content measurements in soils [13, 14, 15] and porous materials in general [16], liquid level monitoring [17, 18], electrical conductivity measurements [19], etc. Generally, in TDR measurements, an EM signal propagates along a SE inserted in the system to be monitored. The response of the system, acquired in terms of reflected signal, is used to retrieve the desired information on the system under test [20].

With regards to the TDR-based leak detection, the basic principles have been described in [10]. However, for the sake of clarity, some important details are also reported herein. It is worth noting that an EM signal travels in a medium different from vacuum, with a specific propagation velocity ( $v$ ) which depends on the geometric and dielectric characteristic of the line. As a consequence, it is useful to introduce the concept of apparent distance,  $d^{app}$ , which is the distance that would be traveled by the EM signal, in the same time interval, if the dielectric medium of the transmission line was air. The direct output of a TDR measurement is a reflectogram, which shows the reflection coefficient ( $\rho$ ) as a function of  $d^{app}$ .

When a leak is present, the reflectogram will show a distinct behaviour in correspondence of the leak. This is due to the fact that water has a high relative dielectric permittivity (approximately equal to 78), which is significantly higher than the typical relative dielectric permittivity of the soil (which is in the order of 3-5).

A detailed description on the analysis and estimation of apparent distances from TDR reflectograms can be found in [21].

With reference to the schematization of Fig. 1,  $B$  and  $E$  indicate the beginning and the end of the SE, respectively, whereas  $L$  indicates the leak. When the TDR signal propagates along the SE, the presence of the leak is typically associated to the variation of  $\rho$  in correspondence of the position of the leak, as shown in Fig. 2 for step-like signal. In particular,  $d_B^{app}$  and  $d_E^{app}$  are the abscissae corresponding to the beginning and to the end of the SE; whereas  $d_L^{app}$  is the apparent distance of the leak.

As detailed in [10], the position of the leak ( $L_L$ ) is evaluated from the reflectograms through the following equation:

$$L_L = \frac{L_L^{app}}{\sqrt{\varepsilon_{eff}}} \quad (1)$$

where  $L_L^{app}$  is the apparent distance of the leak (derived from the TDR reflectogram as reported in [9, 10]) and  $\varepsilon_{eff}$  is the effective dielectric permittivity of the propagation medium (i.e., the soil plus the dielectric insulator between the wires of the SE). In particular, because of its proximity to the wires of the SE, the

permittivity of dielectric insulator has the most significant effect on the  $\varepsilon_{eff}$  value; this means that, even passing from dry soil to water-saturated soil, the resulting variation of  $\varepsilon_{eff}$  is not high. Still, the  $\varepsilon_{eff}$  variation due to the presence of a leak is sufficient to lead to a local change of  $\rho$  in the reflectogram in correspondence of the leakage point.

The value of  $\varepsilon_{eff}$  can be expressed as a function of the actual length and of the apparent length of the SE. Hence, equation (1) can also be expressed as follows:

$$L_L = \frac{L_L^{app}}{(L_{SE}^{app}/L_{SE})} = \frac{d_L^{app} - d_B^{app}}{(d_E^{app} - d_B^{app})/(d_E - d_B)} \quad (2)$$

where  $L_{SE}^{app}$  and  $L_{SE}$  are the apparent and the actual lengths of the SE, respectively.

As detailed in [10], the values of  $d_B^{app}$ ,  $d_E^{app}$ , and  $d_L^{app}$  are to be determined from the reflectogram of the SE, and they are best inferred from the first derivative of the reflectogram. In fact, the derivative better emphasizes the impedance variations, and hence the variation of  $\rho$ . Equation (1) has been implemented in an algorithm (specifically developed by the authors) that provides in real time the estimated value of  $L_L$ .

On a side note, it should be emphasized that the presence of the leaked water changes the dielectric permittivity of the soil locally (around the leak point); but it has a minimal effect on the overall  $\varepsilon_{eff}$  value calculated along the SE. In practice, on a typical length of  $L_{SE} = 100$  m, in presence of an abundant leak, a maximum variation lower than 5% is to be expected for the  $L_{SE}^{app}$  value.

Also, due to its geometric configuration, the SE is sensible to dielectric changes that occur in its immediate proximity. Therefore, since the SE is buried together with the pipe at a depth of at least 80 cm - 120 cm from the road surface, no significant changes (due, for example, to possible seepage of water from the road surface) are expected to occur in proximity of the SE. The proposed system results mostly sensitive only to water presence caused by possible leaks deriving from the pipe-fault in close proximity to the SE.

### 3. Description of the enhancement features of the system

#### 3.1. Configuration of the SE

In the original version of the TDR-based leak localization system, a simple bi-wire was used as SE [10]. In [11], it was described that the very first step for the implementation of the system was to establish (on the blueprint of the pipe network, before the installation of the pipes) the exact length of each SE and the exact position of the corresponding inspection well. The SE's were then to be provided to the construction workers in rolls of pre-established length. This was done because for applying (1) it is necessary to know the exact length of the buried SE.

To avoid this design step, in this work, the use of a different configuration of the SE is proposed an experimentally tested. In particular, a two-element cable configuration is proposed and tested experimentally: Fig. 3.1 shows the schematization of the cross section. It consists of a metallic wire (W1) and of an RG59 coaxial cable, which are mutually insulated and run parallel to each other.

For the considered application, the two-element cable is employed as follows: the outer conductor of the RG59 is used as the reference ground, alternatively, for the inner conductor of the RG59 or for the wire. As detailed in the following, the former configuration serves only to determine the length of the buried SE, whereas the latter configuration serves as SE to localize the position of the leak. Thanks to the presence of a switch in the connector, when the operator connects the TDR instrument to the two-element cable, he/she can decide to propagate TDR signal either along the RG59 or along the bifilar transmission line that is formed between the RG59 outer conductor and the wire.

By propagating the TDR signal through the RG59, because the dielectric characteristics of the RG59 are known, by acquiring the reflectogram corresponding to the RG59, it is possible to retrieve from the reflectogram the actual length of the RG59 (and hence of the SE) even after they are buried by applying the well-known TDR equation:

$$L_{\text{coax}} = \frac{L_{\text{coax}}^{\text{app}}}{\sqrt{\varepsilon_{\text{diel}}}} = \frac{d_E^{\text{app}} - d_B^{\text{app}}}{\sqrt{\varepsilon_{\text{diel}}}} = L_{\text{SE}} \quad (3)$$

where  $L_{\text{coax}}$  is the actual length of the RG59 coaxial cable, and  $\varepsilon_{\text{diel}}$  is the dielectric permittivity of the dielectric insulator of the RG59. Clearly, for (3), the quantities  $d_E^{\text{app}}$  and  $d_B^{\text{ppp}}$  are to be evaluated from the reflectogram of the RG59 cable.

This step allows avoiding the need to pre-establish the exact length that each SE must have, and thus the apparent lengths of the SE with respect to the actual one. During the installation of the pipe, the pipeline workers can install the two-element cable and cut it off at any desired length, thus expediting and simplifying the installation phase.

With reference to Fig. 1, the whole two-element cable (from point  $C$  to point  $E$ ) remains permanently buried; whereas the cable section  $O - C$  is necessary to connect the TDR instrument to the buried cable. It is important to mention that, from point  $C$  to  $E$ , the same type of two-element cable is used. However, the useful portion of the SE is the section between  $B$  and  $E$ .

Finally, with reference to the schematization of Fig. 1, in correspondence of point  $B$ , an Identification (ID) circuit is inserted, namely the DS2401 manufactured by Maxim Integrated. This circuit generates a unique ID number, which is acquired automatically when the operator connects the TDR instrument to the connector emerging from the inspection well. This ID number is associated, via software, to all the information and to the history of the pipe.

### 3.2. Employment of a different connection modality

One additional improvement to the TDR-based leak detection system relates to the type of connector employed for the connection of the TDR instrument to the SE. In the previous configuration of the system [11], traditional electrical connectors had been used. In particular, in the inspection well, two connectors were present: one to propagate the signal through the SE, and the other to acquire the ID code of the DS2401. Additionally, to protect the connectors from the environment, they were enclosed in a plastic box. In this work, instead, the use of a single, ingress protected (IP) type of connector is proposed. This type of connector has a cap that can protect the connector when it is not used, also it is water-proof and dust-proof. As a result, this connection modality is much more resistant to stressful environmental conditions. The used connector, which is shown in Fig. 4, has five pins: two are relative to the ID circuit (signal and ground); one is for the signal pin of the RG59; one is for the signal pin for the SE; and, finally, one is the reference ground pin, for the SE and for the RG59.

### 3.3. TDR instrument

To assess the possibility of further increasing the cost-effectiveness of the TDR-based leak localization system, the possibility of employing a lower-cost TDR instrument was considered. To this purpose, also experimental tests were carried out by comparatively using two TDR instruments, differing in specifications and costs, to identify the position of a leak.

Currently, the TDR instrument that has been used for leak detection is the HL1500: a portable, battery-powered TDR unit produced by Hyperlabs Inc. [22]. The HL1500 generates a step-like signal with a rise time

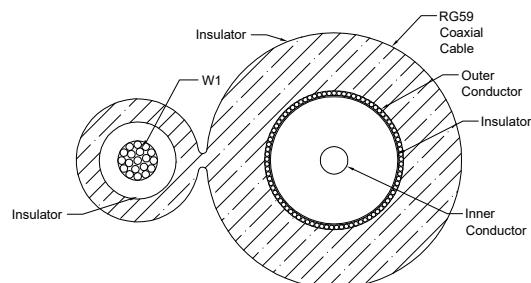


Figure 3: Cross section of the two-element cable used in this work: it consists of an insulated metallic wire (*left*) and of an RG59 coaxial cable (*right*).

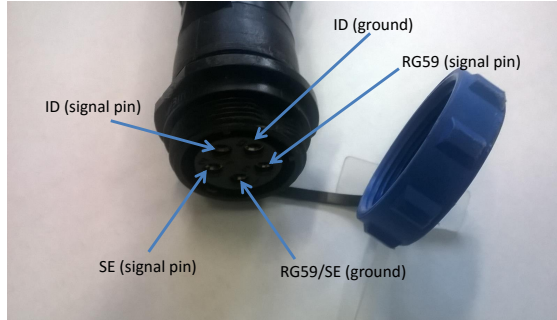


Figure 4: IP Connector used at the beginning of the SE.

Table 1: Specifications of the two considered TDR instruments

	HL1500	TDR-307usb
Type of signal	step-like	pulse
Characteristics of the signal	Rise time 200 ps	pulse width from 10 ns to 50 $\mu$ s
Amplitude of the signal	250 mV	10 V (on matched load)
Output impedance	50 $\Omega$	ranges from 25 to 600
Power	12 V battery	USB port

of 200 ps; the amplitude of the signal is 250 mV and the output port of the instrument is 50  $\Omega$ -matched. The HL1500 is a high-performing piece of equipment, which is widely used not only for in-the-field applications, but also for laboratory measurements.

In view of lowering the cost, the other TDR instrument that was tested for leak-detection application is the TDR-307usb (manufactured by Ersted Zao): this TDR instrument has a simpler architecture, and its cost is approximately 1/4 of that of the HL1500. The TDR-307usb generates a pulse signal and is powered through a USB port.

Table 1 summarizes the specifications of the two considered instruments. As detailed in the following, the performance of these two TDR instruments was assessed by comparatively using them for the localization of a leak in a pipe section.

#### 4. Description of the implementation steps

This section describes in detail all the steps that should be followed for preparing the pipe networks for the successive inspection through the TDR-based leak-localization system.

##### 4.1. Installation of the two-element cable

The installation of the two-element cable is carried out concurrently with the installation of the pipes. After excavation, the cable is positioned along the trench (Fig. 5(a)). Successively, the pipe is installed (as shown in Fig. 5(b)) and is buried with the SE. As already mentioned, thanks to the presence of the RG59 cable, there is no need to establish in advance the length of the SE. One end of the two-element cable must emerge through an inspection well (as shown in Fig. 1) to allow the connection to the TDR instrument.

##### 4.2. Initialization and georeferencing of the SE

Once the pipe and the two-element cable have been installed, the SE's are initialized. This step is not mandatory, but it makes the subsequent leak-detection activity and the overall management of the leak-detection activity much more effective and efficient.



Figure 5: Installation of the two-element cable (a); Installation of the pipe (b).

The operator goes on site and connects the TDR instrument to the IP connector in the inspection well. The dedicated software automatically acquires the ID code and displays a window a table to be filled: the operator enters the basic information (e.g., street name, GPS coordinates, etc.). All this information is stored in the database, and is available (and automatically retrievable) for the subsequent inspections. This phase can be considered as the geo-tagging of the SE's. In view of large-scale implementation of the system, the developed software was equipped with several tools for the preparation for the database, periodic updates, historical comparisons, etc. and for the integration with other management platforms.

Via software, the operator evaluates the length of the buried SE. To this purpose, via software, he/she selects to propagate the TDR signal through the RG59 coaxial cable. Once the reflectogram of the RG59 is acquired (in less than two minutes), the software automatically calculates the actual length of the RG59 and of the SE. The evaluated length of the SE,  $L_{SE}$ , is stored in the database as part of the identification information of that inspection well/SE.

Finally, once again via software, the operator selects to propagate the TDR signal along the SE; and he/she acquires and stores the corresponding reflectogram. This reflectogram represents the *electromagnetic signature* of the SE in normal operating condition of the pipe. Acquiring the reflectogram right after the installation and storing it in a database associated to the specific pipe section, serves as a reference to which compare the reflectograms acquired subsequently, during pipe inspection.

#### 4.3. Use of the system

To check for the presence of leaks, the operator goes on site and connects the TDR instrument to the IP connector in the inspection well, as shown in Fig. 6(a). Thanks to the presence of the ID circuit, the dedicated software automatically calls up all the data that have been stored in the initialization steps and in previous inspections.

The operator propagates the TDR signal through the SE, and acquires the corresponding reflectogram. The software directly provides the position of the leak as distance from the inspection well. As shown in Fig. 6(b), thanks to the GPS coordinates acquired during the installation phase, the developed software can directly launch a satellite view, displaying the map of the site. The software indicates with two markers in correspondence of the beginning and of the end of the SE. In presence of a leak, the software also displays a third marker in correspondence of the estimated GPS coordinates of the identified leak.

On a side note, it is worth mentioning that the installation of the SE's in the underground pipes brings another important advantage (in addition to the intrinsic advantage of the localization of leak when the





Figure 6: Use of the system: (a) Measurement for checking the presence of a leak; (b) Google Earth image showing the position of the pipe under inspection and the position of the leak.

infrastructure is in use). In fact, it is well known that, after the installation of the pipelines is complete, functional tests have to be carried out to verify the correct installation of the pipes (e.g. no broken pipes after burial, no damaged seals between the pipes, etc.). In this regard, these functional tests can be carried out employing TDR and the installed SE's: in fact, TDR measurements will directly localize the position of possible pipe installation problems.

## 5. Experimental tests

To test the system and the two TDR instruments, a two-element cable with length  $L_{SE}^{ref} = L_{coax}^{ref} = 100.0$  m was installed on a pipe. The presence of a leak was simulated through a gate valve inserted between two section of pipes: by opening and closing the gate valve through a manhole, water was leaked intentionally from the pipe. The gate valve (and, hence, the leakage point) was set at a reference distance of  $L_L^{ref} = 65.3$  m from the inspection well.

### 5.1. Evaluation of the length of the buried SE

First, to test the system, the length of the buried SE was evaluated (as it had been unknown) through the procedure described in Section 3.

Fig. 7(a) shows the reflectogram acquired through the HL1500 for the RG59 cable and its first derivative; the beginning ( $B$ ) and the end ( $E$ ) of the RG59, in fact, are identified through the analysis of the reflectogram and from the peaks of the derivative. After the steep portion of the reflectogram, the first horizontal portion up to point  $C$  corresponds to the cable used for connecting the TDR instrument to the IP connector; because of the slight impedance mismatch between connectors, at this point, there is a relative maximum of the first derivative. Then, the portion between  $C$  and  $B$  represents the cable section between the IP connector and the beginning of the SE ( $d_B^{app} = 10.6$  m). Finally, the end of the RG59 corresponds to the abrupt change of  $\rho$ , at approximately  $d^{app} = 128.0$  m: this corresponds approximately to the maximum of the first derivative, in correspondence of the same abscissa.

As expected from TDR theory, because the electrical impedance along the RG59 is constant, the corresponding portion of the reflectogram is practically horizontal ( $\rho \cong const$ ). The  $\rho$  variations at  $d^{app} \cong 46.5$  m, 55.7 m, and 101.0 m are due to the multiple reflection effects caused by the connections.

From specifications, for the RG59, the value of  $v/c$  is 0.85 (where  $c$  is the speed of light in vacuum and  $v$  is the propagation velocity in the coaxial cable). By applying (3), the estimated length of the SE was 99.8 m, which is in optimal agreement with the known value of  $L_{SE}^{ref}$ .

For the sake of comparison, a similar procedure was carried out by acquiring the reflectogram of the RG59 through the TDR-307usb (Fig. 7(b)). The first peak (at  $d^{app} = 9.8$  m) corresponds to the incident

pulse signal. The point  $C$  and the point  $B$  are identified by acquiring the reflectogram while the cable is being assembled in laboratory. The peak at  $d^{app} = 134.3$  m corresponds to the end of the RG59 cable. The corresponding evaluated length of the buried two-element cable was 99.5 m. Also in this case, the multiple reflection effect is present. Also, some minor variations in the TDR-307usb reflectogram are caused by noise and resolution limits of the instrument.

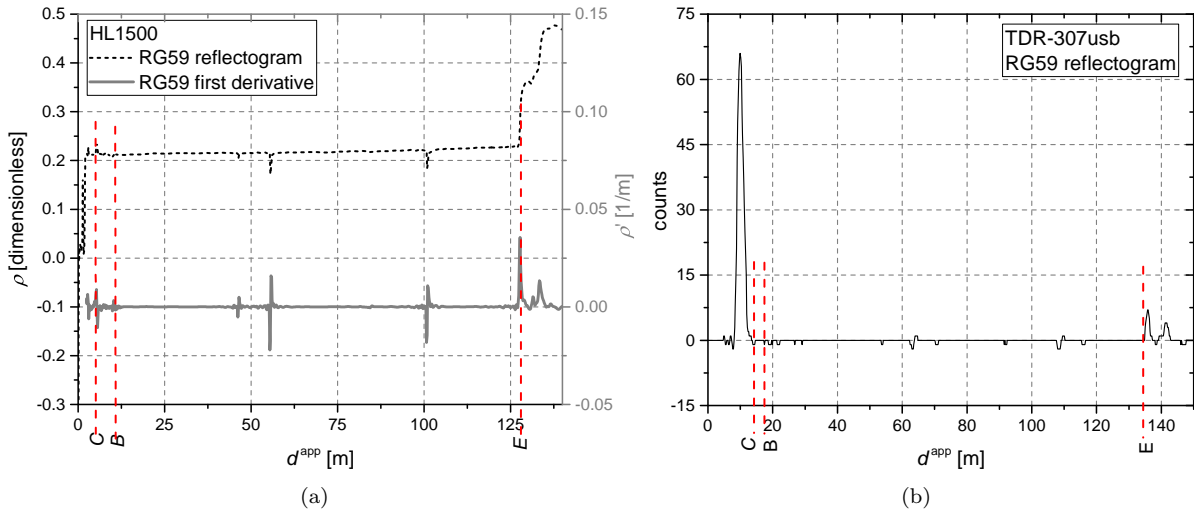


Figure 7: Reflectogram acquired for the RG59, through the HL1500 (a) and through the TDR-307usb (b). For the HL1500 measurement, also the first derivative of the reflectogram is reported.

It should be noted that to compare directly the abscissae of the reflectograms obtained through the HL1500 and of the TDR-307usb, it should be necessary to identify to a specific/known impedance mismatch, and shift the two reflectograms so that these points coincide in the two graphs. In the case of the results of Fig. 7(a) and Fig. 7(b), the reference point that could be taken as reference for the superimposition of the two reflectograms can be the impedance mismatch at point  $B$ .

### 5.2. Localization of the leak

The second part of the experimental test consisted in localizing the position of the simulated leak. To this purpose, with the gate valve closed (i.e., without leak), the *signature reflectograms* were acquired through the HL1500 and through the TDR-307usb. Successively, the gate valve was opened and water began to leak. As the amount of leaked water increased, reflectograms were acquired through the HL1500 and through the TDR-307usb.

Fig. 8(a) shows the reflectograms acquired through the HL1500. The reflectograms refer to three conditions: without leak; when 100 L of water had escaped the pipe; and when 1000 L of water had escaped the pipe (the amount of escaped water was measured through a domestic water meter). The inset of Fig. 8(a) shows a zoom of the portion of the reflectograms in correspondence of the leak. Fig. 8(b) shows the first derivative of the reflectograms. With reference to Fig. 1, the transition points are also indicated in Fig. 8(b). The variation of  $\rho$  at  $d^{app} \cong 11.0$  m corresponds to point  $B$ . The variation of  $\rho$  for  $d^{app} = 226.0$  m corresponds to the open-circuited termination at the end of the SE. Instead, as expected, in correspondence of  $d^{app} \cong 154.2$  m the reflectograms (in presence of the leak) show the typical minimum associated to the leak. By processing the obtained reflectogram through the developed algorithm (which also implemented (1)), the position of the leak was found to be at 66.5 m of distance from the inspection well; in optimal agreement with the (known) position of the gate valve that had caused the leak (which was  $L_{L,ref} = 65.3$  m).

Similarly, Fig. 9 shows the reflectogram acquired through the TDR-307usb: the inset in the figure shows a zoom of the portion of the reflectograms in correspondence of the leak. The first important observation is that, because for this instrument the TDR test signal is a pulse signal, the TDR-307usb reflectograms

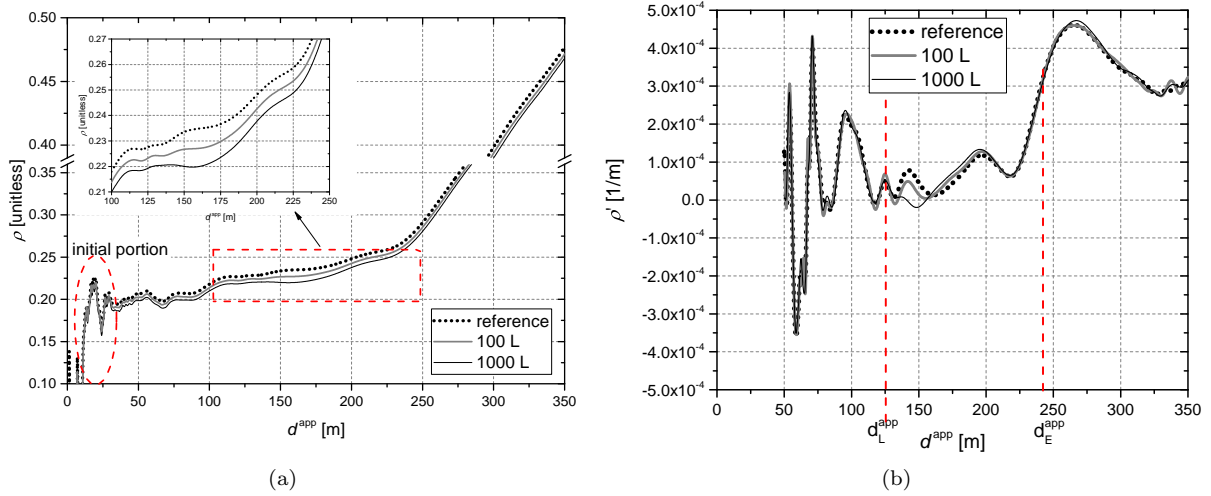


Figure 8: Comparison between the reflectograms acquired through the HL1500, with and without leak present (a); first derivative of the reflectograms (b).

closely resemble the first derivative of the HL1500 reflectograms shown in Fig. 8(b).

For this instrument, to localize the position of the leak, it is particularly useful to compare the reflectogram

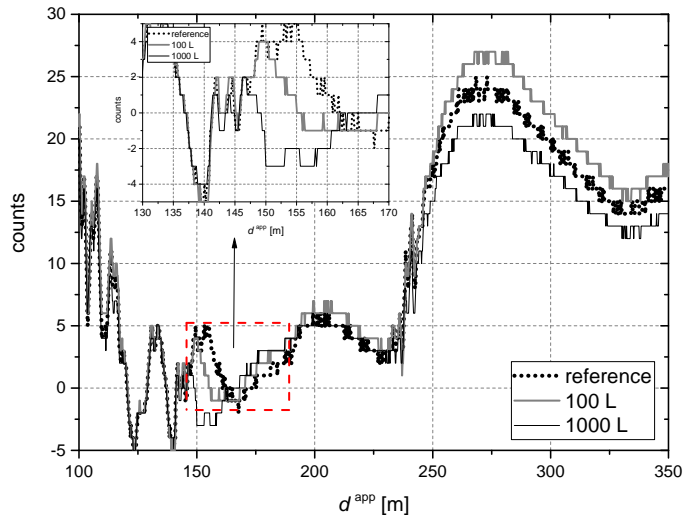


Figure 9: Comparison between the reflectograms acquired through the TDR-307usb, with and without leak present.

in presence of leaks to the signature reflectogram and see where the reflectograms differs from one another. It can be seen that also in this case, the three reflectograms are practically superimposed until  $d^{app} = 150$  m, which corresponds approximately to the apparent distance of the leak.

As for the end of the SE, similarly to the HL1500, it occurs in correspondence of the 'elbow' before the last peak. By applying (1), the position of the leak was estimated  $L_L = 66.5$  m.

Table 2 summarizes the obtained results; the table also reports the absolute error in the estimation of the length of the SE ( $|Err_{SE}|$ ) and of the position of the leak  $|Err_L|$ , for the HL1500 and for the TDR-307usb (calculations were performed on the 1000-L reflectograms). The obtained results show that, in spite of its simpler architecture and lower cost, the TDR-307usb successfully identifies the position of the leak, with an

Table 2: Summarized results obtained through the two considered TDR instruments

	$L_{SE}^{ref}=L_{coax}^{ref}$ [m]	$L_{SE}^{eval}=L_{coax}^{eval}$ [m]	$ Err_{SE} $ [m]	$L_L^{ref}$ [m]	$L_L^{eval}$ [m]	$ Err_L $ [m]
HL1500	100.0	99.8	0.2	65.3	66.5	1.2
TDR-307usb	100.0	99.5	0.5	65.3	66.5	1.2

uncertainty comparable to the one provided by the HL1500.

It is worth mentioning that, in the acquired reflectograms, the differences between different conditions are not particularly evident because, overall, the amount of water intentionally leaked is relatively small compared to the amount of water that leaks from an actual fault.

It should be noted that the different performance of the two instruments in the localization of the leaks, is to be attributed mostly to the sampling time of the TDR-307usb, which leads to a lower resolution. However, differently from the HL1500, the TDR-307usb is more rugged and therefore more suitable for practical applications. Furthermore, the gain functionality of the TDR-307usb anticipates the possibility of employing this instrument also for much longer SEs: this would mean that fewer inspection wells would be needed, as one single SE could be even a kilometer long.

## 6. Conclusions

In this paper, the TDR-based leak detection system and the recent enhancements were presented. In particular, the possibility of using a SE in a different configuration and the employment of a different electrical connection modality were investigated. In particular, it was shown that the former allows to avoid the need to pre-establish (prior to the installation) the length of each SE and the position of the inspection well. The latter allows to expedite the leak-detection activity (as only one connector is used) and to avoid using large IP boxes, and hence of large inspection well. Additionally, all the practical steps for the large-scale implementation of a TDR-based system for water leak detection in underground pipes were presented. Finally, in view of further increasing the cost effectiveness of the system, experimental tests were performed to verify the possibility of employing lower-cost TDR instrumentation. Results demonstrate that the low-cost TDR-307usb can provide adequate measurement accuracy in comparison with its more expensive counterpart, the HL1500.

The system, in this enhanced configuration, represents a powerful and simple solution for the systematic monitoring of health of pipelines.

## References

- [1] Towards efficient use of water resources in Europe, Tech. rep., European Environment Agency.
- [2] M. Farley, S. Trow, Losses in water distribution networks, 2003.
- [3] European benchmarking co-operation — learning from international best practices, Tech. rep., 2012 Water & Wastewater Benchmark (2012).
- [4] EU reference document good practices on leakage management WFD CIS WG PoM, Tech. rep., European Union (2015).
- [5] D. G. für Internationale Zusammenarbeit (GIZ) GmbH (Ed.), A focus on pressure management - Guidelines for water loss reduction, Eschborn, Germany, 2011, Ch. 1, p. 32, supported by UN-Water Decade Programme for Capacity Development (UNW-DPC).
- [6] Z. Liu, Y. Kleiner, State of the art review of inspection technologies for condition assessment of water pipes, Measurement 46 (1) (2013) 1–15. doi:10.1016/j.measurement.2012.05.032.
- [7] R. Li, H. Huang, K. Xin, T. Tao, A review of methods for burst/leakage detection and location in water distribution systems, Water Science and Technology: Water Supply 15 (3) (2015) 429–441. doi:10.2166/ws.2014.131.
- [8] R. Puust, Z. Kapelan, D. Savic, T. Koppel, A review of methods for leakage management in pipe networks, Urban Water Journal 7 (1) (2010) 25–45. doi:10.1080/15730621003610878.
- [9] A. Cataldo, G. Cannazza, E. De Benedetto, N. Giaquinto, Experimental validation of a tdr-based system for measuring leak distances in buried metal pipes, Progress in Electromagnetics Research 132 (2012) 71–90.

- [10] A. Cataldo, E. De Benedetto, G. Cannazza, N. Giaquinto, M. Savino, F. Adamo, Leak detection through microwave reflectometry: From laboratory to practical implementation, *Measurement* 47 (1) (2014) 963–970. doi:10.1016/j.measurement.2013.09.010.
- [11] A. Cataldo, E. De Benedetto, G. Cannazza, A. Masciullo, N. Giaquinto, G. D’Aucelli, N. Costantino, A. De Leo, M. Miraglia, Large-scale implementation of a new TDR-based system for the monitoring of pipe leaks, in: XXI IMEKO World Congress ”Measurement in Research and Industry, 2015, pp. 254–263.
- [12] C. Furse, Reflectometry for structural health monitoring, *Lecture Notes in Electrical Engineering* 96 (2011) 159–185.
- [13] S. Susha Lekshmi, D. Singh, M. Shojaei Baghini, A critical review of soil moisture measurement, *Measurement* 54 (2014) 92–105. doi:10.1016/j.measurement.2014.04.007.
- [14] T. Pastuszka, J. Krzyszczyk, C. Sławiński, K. Lamorski, Effect of time-domain reflectometry probe location on soil moisture measurement during wetting and drying processes, *Measurement: Journal of the International Measurement Confederation* 49 (1) (2014) 182–186. doi:10.1016/j.measurement.2013.11.051.
- [15] N. Giaquinto, A. Cataldo, G. M. D’Aucelli, E. De Benedetto, G. Cannazza, Water detection using bi-wires as sensing elements: Comparison between capacitance-based and time-of-flight-based techniques, *IEEE Sensors Journal* 16 (11) (2016) 4309–4317. doi:10.1109/JSEN.2016.2540299.
- [16] R. Cerny, Time-domain reflectometry method and its application for measuring moisture content in porous materials: A review, *Measurement* 42 (3) (2009) 329 – 336.
- [17] K. Loizou, E. Koutroulis, Water level sensing: State of the art review and performance evaluation of a low-cost measurement system, *Measurement* 89 (2016) 204 – 214. doi:http://dx.doi.org/10.1016/j.measurement.2016.04.019.
- [18] A. Cataldo, E. Piuze, E. De Benedetto, G. Cannazza, Experimental characterization and performance evaluation of flexible two-wire probes for TDR monitoring of liquid level, *IEEE Transactions on Instrumentation and Measurement* 63 (12) (2014) 2779–2788. doi:10.1109/TIM.2014.2318393.
- [19] E. Piuze, A. Cataldo, G. Cannazza, E. De Benedetto, An improved reflectometric method for soil moisture measurement exploiting an innovative triple-short calibration, *IEEE Transactions on Instrumentation and Measurement* 59 (10) (2010) 2747–2754. doi:10.1109/TIM.2010.2045445.
- [20] Time domain reflectometry theory (2013).
- [21] N. Giaquinto, G. D’Aucelli, E. De Benedetto, G. Cannazza, A. Cataldo, E. Piuze, A. Masciullo, Criteria for automated estimation of time of flight in TDR analysis, *IEEE Transactions on Instrumentation and Measurement* 65 (5) (2016) 1215–1224. doi:10.1109/TIM.2015.2495721.
- [22] TDR100 instruction manual - revision 2/10, Logan, UT, <http://www.campbellsci.com/documents/manuals/tdr100.pdf> (2010).